JHEP|Reports

Patient-derived organoids inform pharmacogenomic vulnerabilities in liver cancer

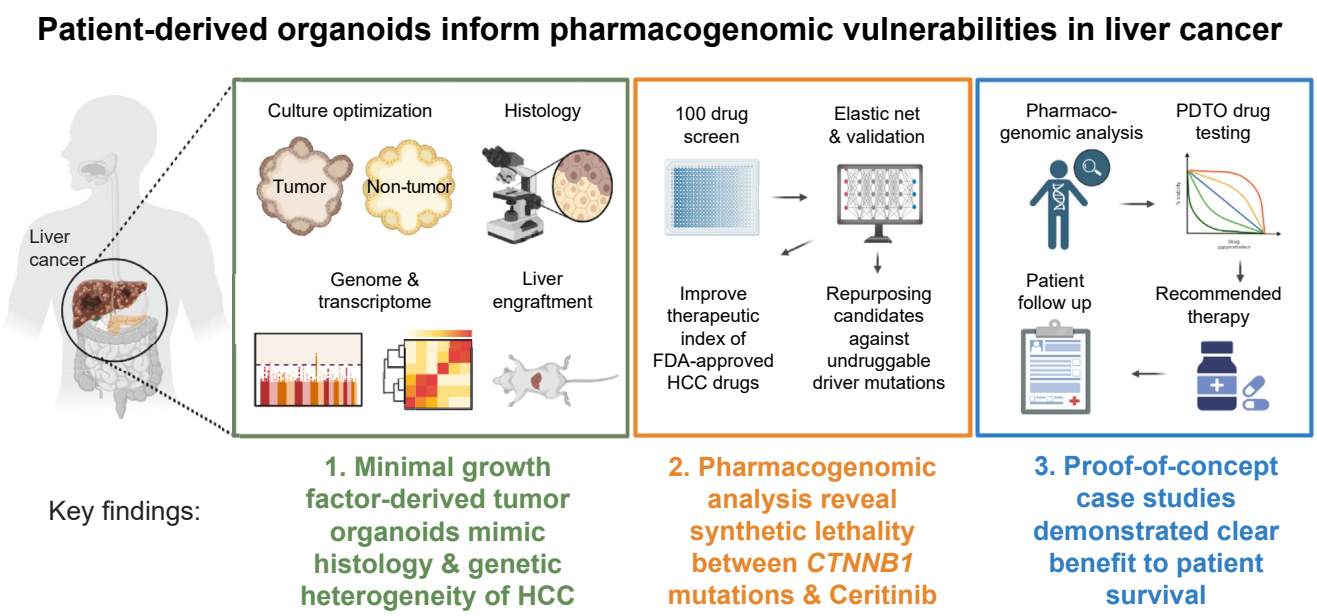
Authors

Alissa Michelle Wong, Hao Huang, Aikha Melissa Wong, …, Xin Wang, Stephen Lam Chan, Nathalie Wong

Correspondence

natwong@cuhk.edu.hk (N. Wong).

Graphical abstract



Highlights:

- Minimal growth factor-derived PDTOs mimic histology and genetic heterogeneity of HCC.
- The majority of tested FDA-approved drugs were not associated with HCC driver mutations.
- *CTNNB1*mut was found to be sensitive to ceritinib via polypharmacological targeting of RPS6KA3.
- The PDTO case study showed clear benefit to patient survival by aiding clinical management.

Impact and implications:

Patient-derived tumor organoids are a reliable model for preclinical and translational studies. Despite positive retrospective correlations with patient response data, challenges such as culture success, cost, standardization, and time constraints hinder their clinical utility in guiding precision medicine. This study underscores the utility of patient-derived organoids established from growth factor-reduced media in many facets of precision oncology, showing for the first time in hepatocellular carcinoma, clear benefit to patient survival in a proof-of-concept case study.

https://doi.org/10.1016/j.jhepr.2025.101426

© 2025 The Author(s). Published by Elsevier B.V. on behalf of European Association for the Study of the Liver (EASL). This is an open access article under the CC BY-NC-ND license (http://creativecommons.org/licenses/by-nc-nd/4.0/).

Research article

JHEP|Reports

Patient-derived organoids inform pharmacogenomic vulnerabilities in liver cancer

Alissa Michelle Wong[1], Hao Huang[2], Aikha Melissa Wong[1], Howard Ho Wai Leung[3], Winnie Wing Yan Cheung[1], Yin Kau Lam[1], Xiaofan Ding[4], Luyao Zhang[1], Clarice Chu[1], Yue Liu[1], Cecilia Ka Wing Chan[1], Anthony Wing Hung Chan[3], Kelvin Kwok Chai Ng[1], Xin Wang[1], Stephen Lam Chan[5], Nathalie Wong[1,*]

JHEP Reports **2025**. vol. 7 | 1–14

Check for updates

Background & Aims: Patient-derived tumor organoids (PDTOs) are a reliable model for preclinical and translational studies. Despite positive retrospective correlations with patient response, challenges such as culture success, cost, standardization, and time constraints hinder their clinical utility in precision medicine. Here, we optimize PDTO establishment using growth factor-reduced media (GF-) to mitigate these challenges and (1) identify somatic variant indicators that can improve the therapeutic index of existing FDA-approved drugs against hepatocellular carcinoma (HCC), (2) elucidate synthetic lethal candidates against undruggable HCC driver mutations, and (3) assess the feasibility of PDTOs in personalized therapy.

Methods: We successfully established a panel of 23 PDTOs from patients with HCC undergoing curative hepatectomy using a protocol primarily based on growth factor-reduced medium. PDTOs were subjected to comprehensive analyses, including the identification of hallmark mutations, assessment of genomic heterogeneity, transcriptomic profiling, and histological characterization. A 100-drug repurposing screen was conducted on the PDTOs and organoids derived from adjacent non-tumoral and normal livers to explore tumor-specific drug responses. Pharmacogenomic analysis using elastic net was performed (cut-off p <0.05) and synthetic lethality links were subject to experimental validation. The clinical relevance of PDTOs in personalized therapy were investigated through two case studies.

Results: Our results reveal that GF-derived PDTOs mimic histology and genetic heterogeneity of HCC. Pharmacogenomic analysis showed that the majority of tested FDA-approved drugs were not associated with HCC driver mutations (<5%). In addition, non-canonical signaling from *CTNNB1* mutations were associated with ceritinib sensitivity (p <0.0001) via polypharmacological targeting of RPS6KA3. The PDTO case study showed clear benefit to patient survival by aiding clinical management.

Conclusions: Our findings underscore the utility of PDTOs established from minimal GF media in many facets of precision oncology advancements.

© 2025 The Author(s). Published by Elsevier B.V. on behalf of European Association for the Study of the Liver (EASL). This is an open access article under the CC BY-NC-ND license (http://creativecommons.org/licenses/by-nc-nd/4.0/).

Introduction

Hepatocellular carcinoma (HCC) is among the leading causes of cancer mortality worldwide.[1] Despite a steady increase in incidence in recent years,[2] only a fraction of patients benefits from current treatments. This is largely attributed to limited actionable clinical variant indicators (CVIs)[3,4] in the HCC genome (Fig. S1A). At best, these alteration–drug matches are suspected to improve outcome based on clinical trials in other tumor types with similar molecular alteration, the status of which is unknown in HCC.[4,5] Dominant HCC mutational drivers, such as *TP53* and *CTNNB1* (β-catenin), also remain undruggable.[6–8] Repurposing of existing drugs with known safety profiles for cancer and non-cancer indications to target synthetic lethal avenues underlying these somatic mutations could be a possible solution to improve therapeutic outcome.[9,10]

Recent 3D culture for patient-derived tumor organoids (PDTOs) has led to the development of more physiologically relevant human cancer models for studies on tumor biology and new therapeutic uses of existing and investigational drugs.[11–13] Despite recent positive retrospective correlations with response data from patients with HCC,[14] methodological challenges such as culture success, cost, standardization, and time constraints hinder their clinical utility in guiding precision medicine.

In this study, we present a culture method that enabled HCC PDTOs to be established using minimal growth factors or conditioned media commonly used in organoid establishment[14–18] in an effort to minimize confounding factors during drug screen and environmental niche dependency.[13,19,20] The reduced reliance on such components is also an important step towards standardization and cost reduction – a major challenge

* Corresponding author. Address: Department of Surgery, The Chinese University of Hong Kong, Prince of Wales Hospital, Shatin, N.T., Hong Kong, China. Tel.: +852-3505-2643, Fax: +852-2637-7974.
E-mail address: natwong@cuhk.edu.hk (N. Wong).
https://doi.org/10.1016/j.jhepr.2025.101426

in making PDTOs accessible and scalable for clinical implementation in the future. We evaluated the efficacy of this approach in establishing HCC PDTOs representing a broad spectrum of histological and genetic profiles, mirroring the somatic mutation frequencies observed in diverse groups of patients with HCC. In parallel, patient-derived tumor cell lines (PDTCLs) from the same parental HCC tumor were also established, and compared head-to-head with the corresponding PDTO for their drug responses in a high-throughput screen. A 100-drug repurposing screen (85 FDA-approved and 15 pipeline drugs) with bioinformatic analysis for somatic variant–drug association was performed to reveal indicators that can improve the therapeutic index of existing HCC treatments, and pharmacogenomic vulnerabilities for undruggable driver mutations, such as *CTNNB1* exon 3 hotspot mutations. Corroboration of tumor specificity and implications on hepatoxicity was performed in matching patient-derived adjacent nontumor (PDNT) and patient-derived normal liver (PDNL) organoids. Finally, we present a proof-of-concept study on PDTO-guided off-label drug use in two patients with advanced inoperable HCC. The positive outcome highlights the predictive value and clinical relevance of PDTO findings in supporting patient management.

Materials and methods

Clinical specimens

Human HCC tumor and adjacent nontumor liver tissues were collected from patients who underwent curative hepatectomy at the Prince of Wales Hospital (PWH), Hong Kong. All cases have been histologically reviewed and confirmed by experienced liver pathologists (Table S1). Informed consent was obtained from all recruited patients and the study procedure was approved by The Joint Chinese University of Hong Kong-New Territories East Cluster Clinical (CUHK-NTEC) Clinical Research Ethics Committee (CREC Ref. No. 2020.420).

Patient-derived organoids establishment

HCC tumor and adjacent nontumoral liver organoids were established from fresh tissues excised from patients with HCC. The detailed protocol is given in the Supplementary Materials & methods section. In brief, tissues were immersed in transport medium upon collection. Tissues were mechanically minced and enzymatically digested with 225 U/ml collagenase type II (Worthington Biochemical Corporation, USA) at 37 °C for 15–30 min.[21,22] Cell clusters were then filtered through a 100-μm cell strainer and seeded in reduced growth factor Matrigel (Corning, USA). Matrigel was solidified in an incubator at 37 °C for 10 min before adding their respective culture media. Tumor organoids were cultured in either growth factor-reduced (GF-) media or growth factor-supplemented (GF+) media (Table S2). Adjacent nontumor liver organoids were cultured in growth factor-rich (GF++) media, as previously reported[21] (Table S2). Organoids were incubated at 37 °C in a humidified incubator with 5% CO_2. Culture medium was changed one to two times a week. Despite the use of GF-, retaining half of the media before passaging along with Y-27632 Rho-associated protein kinase (ROCK) inhibitor (Sigma Aldrich, USA) facilitated self-organization and promote growth after passage. Organoids were passaged by TrypLE (Thermofisher Scientific, USA). Incubation time with TrypLE varies and depend on when small clusters could be observed. Digestion as single cells, particularly at early passage will adversely affect success rate. Frozen stocks were prepared with Recovery™ Cell Culture Freezing Medium (Thermofisher Scientific, USA). Details of reagents are listed in Table S2 and the CTAT table.

Statistical analysis

Correlation matrices, volcano plots, growth inhibition curves, IC_{50} and AUC values were generated by GraphPad Prism Software v8 (GraphPad Software, San Diego, CA, USA). Student's *t* tests were used to compare the AUC values of drug response between different groups. The Benjamini-Hochberg method was used to correct for multiple hypotheses testing. The elastic net regression model was created using the R package glmnet to acquire the regression coefficients for all input data in order to analyse drug response associated genomic features.[23] All statistical analyses were performed using R (version 4.0.2, www.r-project.org, R Foundation for Statistical Computing, Vienna, Austria). Clustvis was used to generate PCA, hierarchical cluster and heatmaps.[24] The CTAT table lists all the software and algorithms used for statistical analysis.

Animal and preclinical studies adhere to the ARRIVE (Animal Research: Reporting of *in vivo* Experiments) guidelines. Additional information is listed under the Supplementary data section. All authors had access to the study data and reviewed and approved the final manuscript.

Results

Generation of patient-derived HCC organoids and liver cultures

Resected liver tissues were obtained from 100 Chinese patients who underwent curative surgery for liver cancer at the Prince of Wales Hospital (PWH), Hong Kong. Tumorous tissues were cultured according to method described herein. *Bona fide* HCC pathology could be confirmed in 77 cases, which also shared somatic mutation of the originating tumor in either *TP53* (*e.g.* R249W, G245V, E326Vfs*18), *CTNNB1* (*e.g.* S45P, T41A), or *TERT* promoter (*e.g.* -124C>T, -146C>T) (Table S1). Successful short-term culture (≥8 weeks, less than passage 20) could be achieved for 73/77 cases (94.8%). Although short-term cultures maintained the driver mutations of the matching tumor tissue as well as self-organize through cell–cell and cell–matrix interactions within the initial one to two passages as per organoid definition consensus,[25] the small initial tissue or lower tumor purity results in the presence of fibroblast outgrowth (Table S1). These overtake the tumor organoids soon after three passages and make it difficult to maintain a stable biobank. Regardless, the value of short-term/3D primary culture lies in the clinical application. Drug testing can be achieved within a short turnaround time to inform potentially efficacious and non-efficacious drug treatment options for patient as recently demonstrated in refractory pediatric cancers.[26] However, long-term PDTO culture at more than passage 20[18] was achieved in 23/77 cases (30%). These PDTOs can be expanded, frozen, and thawed for subsequent culture to establish a biobank (Fig. 1A and B, Fig. S1B and C). Cryopreserved PDTOs could be revived from >4 years of storage. The incidence of driver

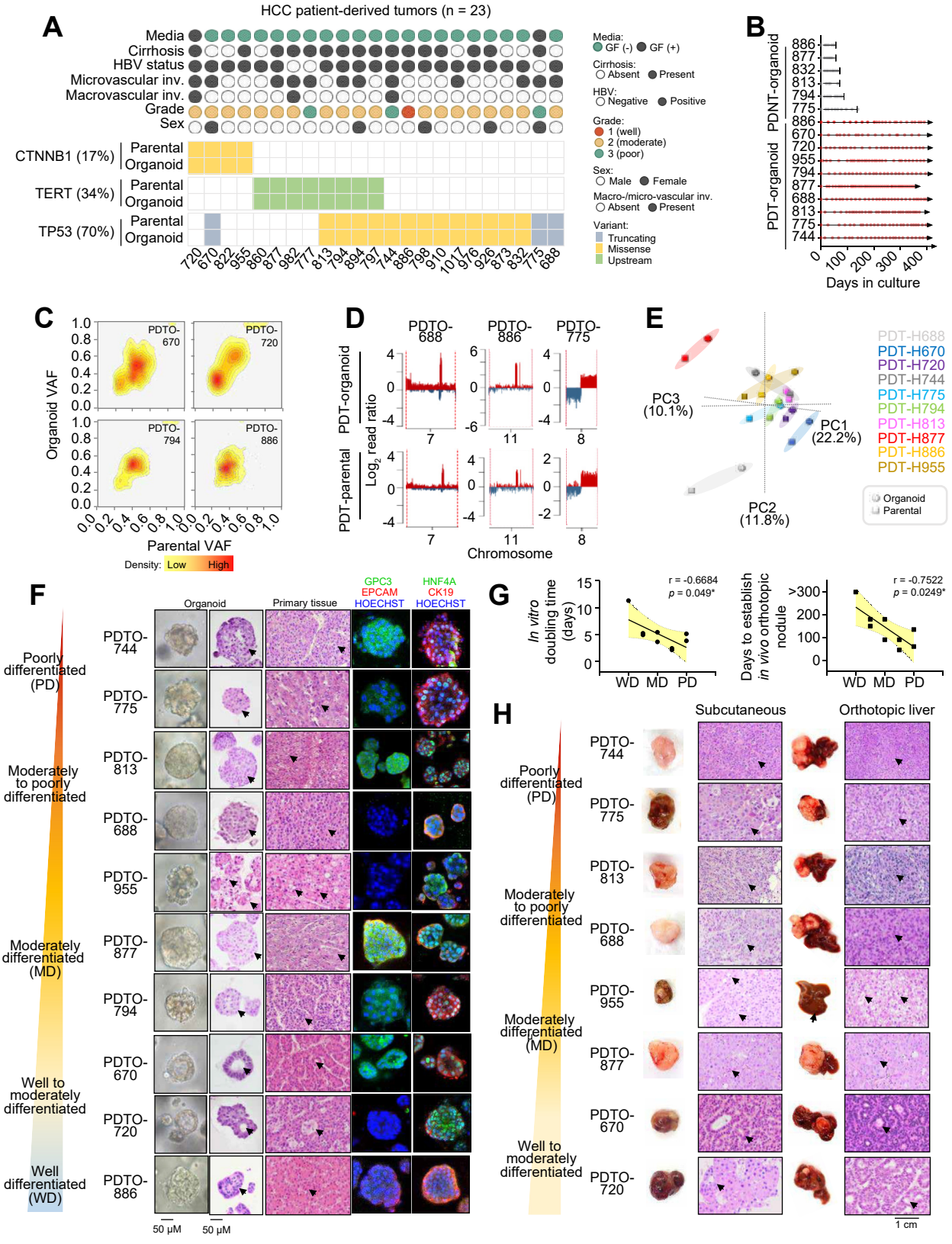


Fig. 1. Patient-derived tumor organoids (PDTOs) recapitulate genomic, transcriptomic, and histological features of their originating parental tumor. (A) Summary of PDTO successes, their clinicopathological information, culture media used, and driver mutation status. (B) Plot of individual patient-derived organoids (PDOs) in culture by days. Each datapoint represents a passage. (C) Contour plot of variant allelic frequency (VAF >0.2) in matching parental tumor and derived organoid (D) Copy number profile highlighting concordant amplification and loss between parental tumor and matching organoid. Examples on chromosomes 7, 11,

mutations among our long-term PDTO cultures are similar to larger HBV-prevalent HCC cohorts, and mutual exclusivity reported between *TP53* and *CTNNB1* were also maintained (p = 0.0331) (Fig. 1A).[22,27,28] A total of 21/23 PDTOs (91.3%) were successfully cultured and expanded in GF- basal medium, whereas the remaining 2/23 (8.7%) required growth factor-supplemented medium (GF+) (Fig. 1A).

In addition to HCC PDTOs, we also generated 10 patient-derived organoids from nontumor (seven PDNT) and normal livers (three PDNL) in GF++ medium as previously reported (Tables S1 and S2). Their non-malignant feature was affirmed by the absence of cosmic mutations and a balanced genome from whole exome sequencing (WES), and the liver origin by positive staining of hepatic differentiation (HNF4α^{+}) and human liver stem/progenitor markers (EpCAM^{+}, CK19^{+}) (Tables S4 and S5, Fig. S2A and B). In parallel to PDTOs, the same parental tumor was also subjected to conventional 2D-monolayer culture for cell line using a protocol previously developed by our group.[29,30] In later drug sensitivity testing, we compared 3D PDTOs with their corresponding 2D patient-derived tumor cell lines (PDTCLs), as well as HCC cell lines from the American Type Culture Collection (ATCC), for drug–response profile.

PDTOs retain histopathology and molecular characteristics of parental tumor

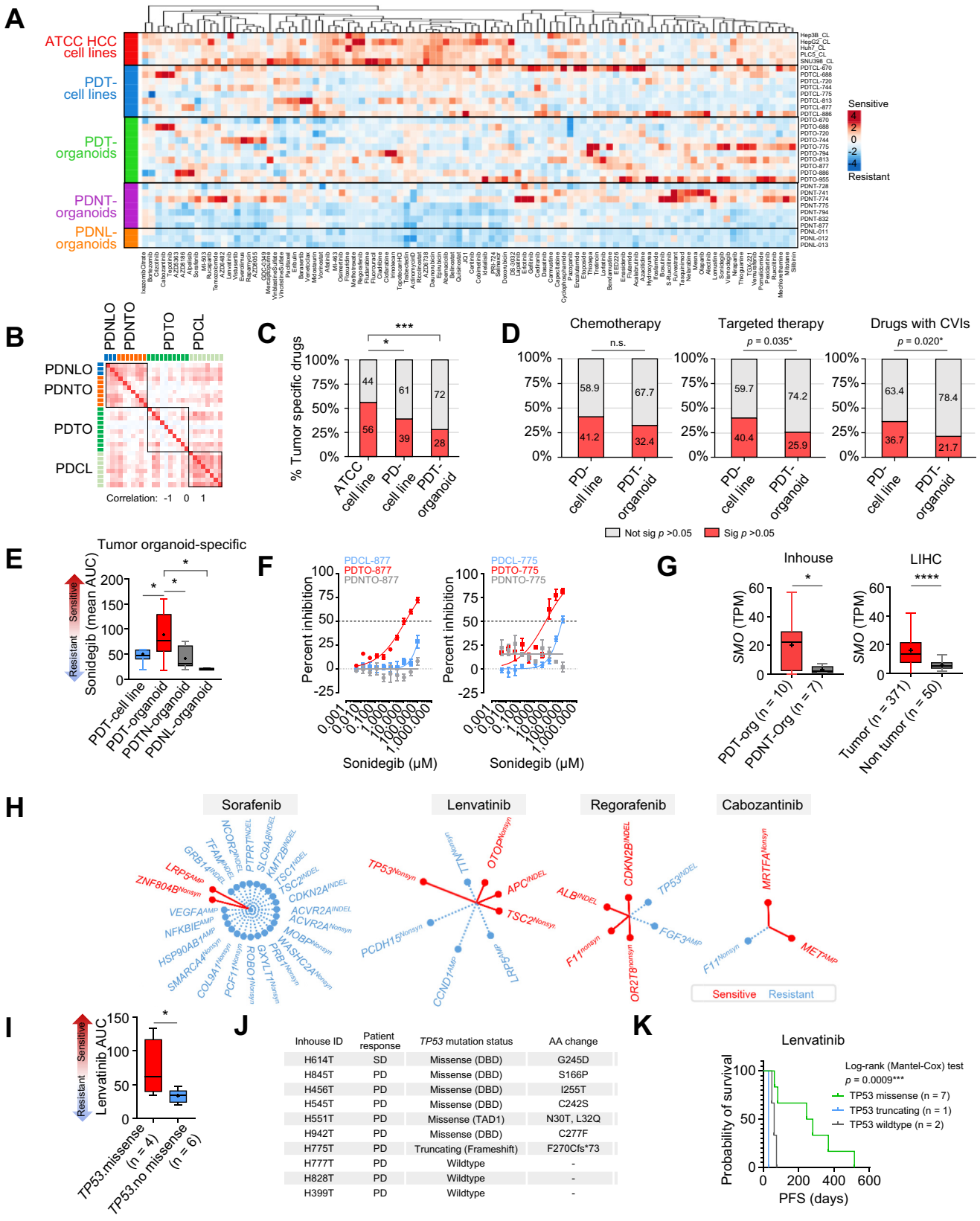
With the goal of generating HCC models that would reflect the biology of a patient's tumor, we performed detailed analysis on 10 PDTO lines that represent different tumor histopathology and harboring major HCC-associated genetic anomalies (Fig. 1A, Fig. S3A). Of note, three patients have paired tumor and adjacent nontumor organoids developed (PD-775, PD-794, PD-877) (Fig. S3B). WES showed pathogenic mutations to be preserved in PDTOs, and tumor heterogeneity based on mutational variant allele frequency (VAF) was also maintained (Fig. 1C). Major clonal fraction in parental tumors was found to be conserved in their corresponding PDTO, for example PDTO-794 and PDTO-886, and this extended to also subclonal fractions, for example those found in PDTO-670 and PDTO-720 (Fig. 1C). In addition to mutations, frequently reported copy number variants (CNVs) such as amplification of chr.11q13.3 (harboring *FGF19, CCND1*) and chr.7q31.2 (harboring *MET, EGFR*), and loss of regional chr.8p21.1 (harboring *DLC1, FZD3*) in parental tumor were retained in PDTO (Fig. 1D, Fig. S3C, Tables S4 and S5). Unsupervised principal component analysis (PCA) of transcriptome datasets readily illustrated a high concordance and clear similarity between parental tumor and derived organoid (Fig. 1E, Table S6). We also noted that while non-malignant liver organoids (PDNT and PDNL) have a finite life span varying between 40 and 150 days (four to 10 passages) before senescing, PDTOs can stably grow beyond 400 days (>40 passages) (Fig. 1B).

Similar to other studies, histological examination of PDTOs also showed that they can recapitulate the original tissue architecture (Fig. 1F). A strong resemblance in several morphological features could be observed such as solid (PDTO-744, PDTO-813), pseudoacinar (PDTO-720), trabeculae (PDTO-794, PDTO-670), steatohepatitic (PDTO-955) and well-differentiated (PDTO-886) tumor patterns (Fig. 1F). PDNT and PDNL organoids, however, consistently displayed a cystic morphology of monolayer epithelium (Fig. S2A). Immunofluorescence (IF) staining of HCC-associated marker GPC3, CK19, and HNF4α showed varying degrees of expression among PDTOs, whereas EpCAM positivity was mainly found in PDNT and PDNL organoids (Fig. 1F, Fig. S2A). *In vitro* doubling time of PDTO cell growth correlated with tumor histopathology grade, where well to moderately differentiated cases have longer doubling times than those of poorly differentiated PDTOs (Fig. 1G). Tumorigenicity of PDTOs could also be confirmed by successful engraftment in an immunocompromised NSG (NOD-*Prkdc*^{scid} *Il2rg*^{em1}/*Smoc*) mouse model, either subcutaneously (9/10 PDTOs) or orthotopically (8/10 PDTOs) (Fig. 1H, Fig. S4A). Of note, the engraftment time for orthotopically injected PDTOs also concur well with tumor histopathology, where poorly differentiated PDTOs could be successfully engrafted orthotopically faster than those of well or moderately differentiated PDTOs (Fig. 1G, Fig. S4A). For PDT-955, steatosis featuring large intracytoplasmic vacuoles and compressed eccentric nuclei, and cells with clear cytoplasm positive for adipophilin were maintained not only in organoids, but also in xenografts (Fig. S4B).[31–33] Overall evidence leads us to believe that our PDTOs established faithfully recapitulate their parental HCC tumor.

Pharmacogenomic indicators for improved therapeutic index

A 100-drug panel consisting of 85 FDA-approved and 15 pipeline drugs targeting pathways that are frequently deregulated in HCC were tested in 28 patient-derived models (10 PDTO, eight PDTCL, seven PDNTO [patient-derived nontumor organoid], and three PDNLO [patient-derived normal liver organoid]) and five HCC cell lines from the ATCC (Table S3). A total of eight PDTCLs (PDTCL-670, -688, -720, -744, -775, -813, -877 and -886) was established from the same originating tissue as the PDTOs. In assessing drug response, the S:B and Z′ factor (>0.5) of minimum and maximum controls were used as internal quality control measures. Normalized percentage inhibition was used to generate AUC and IC_{50} (Table S7). Two independent screens were conducted on each organoid or cell line, and a high concordance between runs was demonstrated (r >0.7, p <0.0001) (Fig. S4C). Of note, drug screen profiles from the same PDTO obtained from early (mean p8) *vs.* late (mean p11) passage showed high concordance and no significant change in drug response (Fig. S4D and E). Among the 100 drugs tested, PDNT and PDNL organoids showed therapeutic resistance to the majority, suggesting many drugs are in fact tumor specific (Fig. 2A). Correlation matrix of mean AUCs

and 8 shown. (E) Unsupervised 3D principal component analysis (PCA) of transcriptome TPM in parental tumor and matching patient-derived (PD) organoid. Colors indicate individual cases of matching parental tumor and organoid. (F) Representative phase contrast, H&E, and immunofluorescence staining of PD-tumor organoids and parental tumor established from well (WD), moderately (MD) to poorly differentiated (PD) HCCs. (G) Spearman correlation plots of PD-tumor organoids doubling time by histopathology grade and rate of *in vivo* engraftment. (H) Representative photos and H&E staining of xenografts from subcutaneous or orthotopic PDTO inoculations. TPM, transcript per million; VAF, variant allele frequency.



Inhouse ID	Patient response	*TP53* mutation status	AA change
H614T	SD	Missense (DBD)	G245D
H845T	PD	Missense (DBD)	S166P
H456T	PD	Missense (DBD)	I255T
H545T	PD	Missense (DBD)	C242S
H551T	PD	Missense (TAD1)	N30T, L32Q
H942T	PD	Missense (DBD)	C277F
H775T	PD	Truncating (Frameshift)	F270Cfs*73
H777T	PD	Wildtype	-
H828T	PD	Wildtype	-
H399T	PD	Wildtype	-

Fig. 2. Pharmacogenomic indicators of therapeutic value. (A) One-way hierarchical clustering of 100 drug response profiles between ATCC (n 5), PD-cell line (n = 8), PDT-organoid (n = 10), PDNT-organoid (n = 7), and PDNL-organoid (n = 3) showed drugs commonly sensitive in ATCC HCC cell lines are more resistant in PDT-cell lines and to a lesser extent in PDT-organoids. (B) Mean AUC Spearman correlation matrix between patient-derived organoids and cell lines. (C) Fisher exact test showed significant decrease in the number of tumor-specific drugs in PDTOs based on comparison with PDTCL and ATCC cell lines (*p <0.05). (D) Percentage of drugs

indicated that response profiles of PDTO were more heterogenous compared with the combined PDNT and PDNL organoids (Fig. 2B). Contrary to PDTO, a more homogeneous response was shown for matching PDTCL cultures (Fig. 2A), suggesting the state of the monolayer has an influence on drug response. Indeed, we found common HCC cell lines from the ATCC showed highest sensitivity to most drugs (Fig. 2C). A clear discrimination between PDTOs and PDTCLs lies in targeted therapies and drugs with CVIs,[3] for example rapamycin and pipeline drug AZD8055 (Fig. 2C, Fig. S5A–D). No significant difference was found for chemotherapies (Fig. 2C).

Major strides have been achieved in identifying actionable clinical variants in many human cancers,[4,5,34] but few have been reported for HCC (Fig. S1A). We investigated the pharmacogenomic landscape by integrating common somatic nucleotide variants (SNVs), recurring CNVs, and drug response data from 100 compounds tested (Fig. S5E). We identified PDTO-specific variant–drug associations, for instance FDA-approved sonidegib (SMO inhibitor) (Fig. 2E), where the drug efficacy was more profound in tumor organoids. This can be clearly demonstrated when matching cases of PDTO, cell line, and nontumor organoid were compared (Fig. 2F). The effect of sonidegib is likely attributable to the significant upregulation of its direct binding target SMO in PDTOs,[35] which is consistent with The Cancer Genome Atlas (TCGA) Liver Hepatocellular Carcinoma (LIHC) data (Fig. 2G). Of interest, a first interventional study of sonidegib (LDE225) in patients with HCC has just completed and is awaiting results to determine if there is any improved clinical outcome (clinical trial no. NCT02151864).

Using elastic net (EN) regression, we identified 1,619 variant–drug predictive pairs (p <0.05) (Table S8). Unfortunately, the majority of variants associated with sensitivity and resistance to existing FDA-approved drugs sorafenib, lenvatinib, regorafenib, and cabozantinib are often passenger mutations or pathogenic mutations reported in <5% of HCCs, which limit their clinical utility (Fig. 2H, Fig. S5F).[6,22,28] For instance, cabozantinib sensitivity towards PDTOs harboring *MET* amplification (*MET*^{amp}) is consistent with its mechanism of action[36] (Figs. 1C, 2H, and Fig. S5G). Although pathogenic, the low incidence of *MET*^{amp} in both our inhouse panel of PDTO (present in PDTO-688 only) and the LIHC TCGA cohort (<3%) may account for the low response rate (Figs. S3A and S5F and G). The only response to lenvatinib were associated with the frequently mutated driver gene *TP53*, whereby missense mutations affect 25% of HCCs (Fig. 2H).[22,27,28,37] EN results revealed that lenvatinib sensitivity correlated with *TP53* missense mutations (Fig. 2H and J).

To substantiate the clinical relevance of these findings, we retrospectively determined the *TP53* mutation status in a cohort of 10 patients with HCC with follow-up information on lenvatinib treatment within our hospital as previously described (Fig. 2J).[38] We adapted an analysis approach similar to that described by Wheler *et al.*[39] in evaluating *TP53* status and response to lenvatinib in our cohort. Patient outcome was assessed and determined by managing oncologist. Among the 10 HCC patients, seven harbored mutant *TP53* (Fig. 2J). Of which, six were missense (five at the DNA-binding domain/DBD and one at the terminal-transactivating domain 1/TAD), and one truncating frameshift (Fig. 2J). The higher incidence of missense over truncating mutations is consistent with previously reported HCC genome studies by us and others.[22,28,37] Although there was no difference in overall patient outcome with only one patient harboring *TP53* DBD missense mutation showing stable disease, there was significant improvement in progression-free survival for patients carrying *TP53* missense mutations (median = 262.5 days) compared with truncating (median = 30 days) and wildtype status (median = 62 days) who received lenvatinib (Fig. 2K). This warrants further investigation in a larger patient cohort to draw firm conclusions between *TP53* missense mutation association with lenvatinib response.

CTNNB1^{mut} sensitivity towards ceritinib is via noncanonical Wnt signal independent of ALK

Pharmacogenomic vulnerabilities associated with major somatic mutations of *CTNNB1* remain elusive in HCC.[3] *CTNNB1* gain-of-function mutations is a top driver in HCC tumorigenesis occurring in 11–37% of cases.[22,28,37] EN analysis in our panel of PDTOs indicate *CTNNB1*mut sensitivity to ceritinib (Fig. 3A). In the extended cohort, *CTNNB1* mutated PDTOs (n = 4) were sensitive to ceritinib compared with wildtype (n = 19) as evidenced by significantly lower IC_{50} in *CTNNB1* mutated (mean ± SD = 5.33 ± 2.74 μM) than *CTNNB1* wildtype PDTOs (mean ± SD = 27.28 ± 19.58 μM) (Fig. 3A–B). Ceritinib also showed low cytotoxic effect in nontumor and normal liver organoids (mean IC_{50} of 45.398 ± 25.136 μM) (Fig. 3B, Table S7), suggestive of its favorable therapeutic index in addition to mutant-bias. Our data showed ceritinib could lead to both *CTNNB1*^{mut}-specific *in vitro* cell death (Fig. 3C and D) and reduction of tumor burden in a *CTNNB1*^{mut} orthotopic *in vivo* model (Fig. 3E).

Ceritinib is FDA-approved for treating *ALK*-positive metastatic non-small cell lung cancer and sensitivity is associated with *ALK* rearrangement/fusion and upregulations.[40,41] Interestingly, no *ALK* fusion and upregulation could be found in *CTNNB1*^{mut} PDTOs or HCC in general (Fig. S6A–C). Overall, findings led us to believe that ceritinib-mediated *CTNNB1*^{mut} growth inhibition is independent of canonical *ALK*. Notably, the study by Kuenzi *et al.*[41] also found ceritinib sensitivity in ALK-negative lung cancer cell lines and uncovered a polypharmacology mechanism involving non-canonical targets, including RPS6KA3 (Ribosomal Protein S6 Kinase A3),

showing tumor specificity among chemotherapy drugs, targeted therapy, and drugs with clinical variant indicators (CVIs). (E) Sonidegib mean AUC boxplot grouped by PD-cell line, PDT-organoid, PDNT-organoid, and PDNL-organoid. Unpaired t test deemed significant if *p <0.05. (F) Sonidegib growth inhibition curves from individual patients with successfully established: PDT-organoid, PDT-monolayer, PDNT-organoid. (G) Sonidegib target *SMO* mRNA expression (TPM) in PDT and NT organoids and TCGA LIHC HCC cohort. (H) Elastic net results for FDA approved sorafenib, lenvatinib, regorafenib and cabozantinib against HCC. Line length is proportional to the p value. (I) Lenvatinib AUC boxplot grouped by *TP53* missense status. Unpaired Student t test *p <0.05, **p <0.01, ***p <0.001. (J) Summary table for *TP53* mutation status of 10 HCC patients with known lenvatinib treatment outcome (Prince of Wales Hospital, PWH n = 10). (K) Progression-free survival analysis of patients who received lenvatinib grouped by their *TP53* mutation status was performed by the Kaplan–Meier method and compared by the log-rank test. ATCC, American Type Culture Collection; AUC, Area under curve; HCC, hepatocellular carcinoma; LIHC, Liver Hepatocellular Carcinoma; NT, nontumor; PD, patient-derived; PDCL, patient-derived cell line; PDNL, patient-derived normal liver; PDNT, patient-derived adjacent nontumor; PDT, patient-derived tumor; PDTO, patient-derived tumor organoid; TCGA, The Cancer Genome Atlas; TPM, transcript per million.

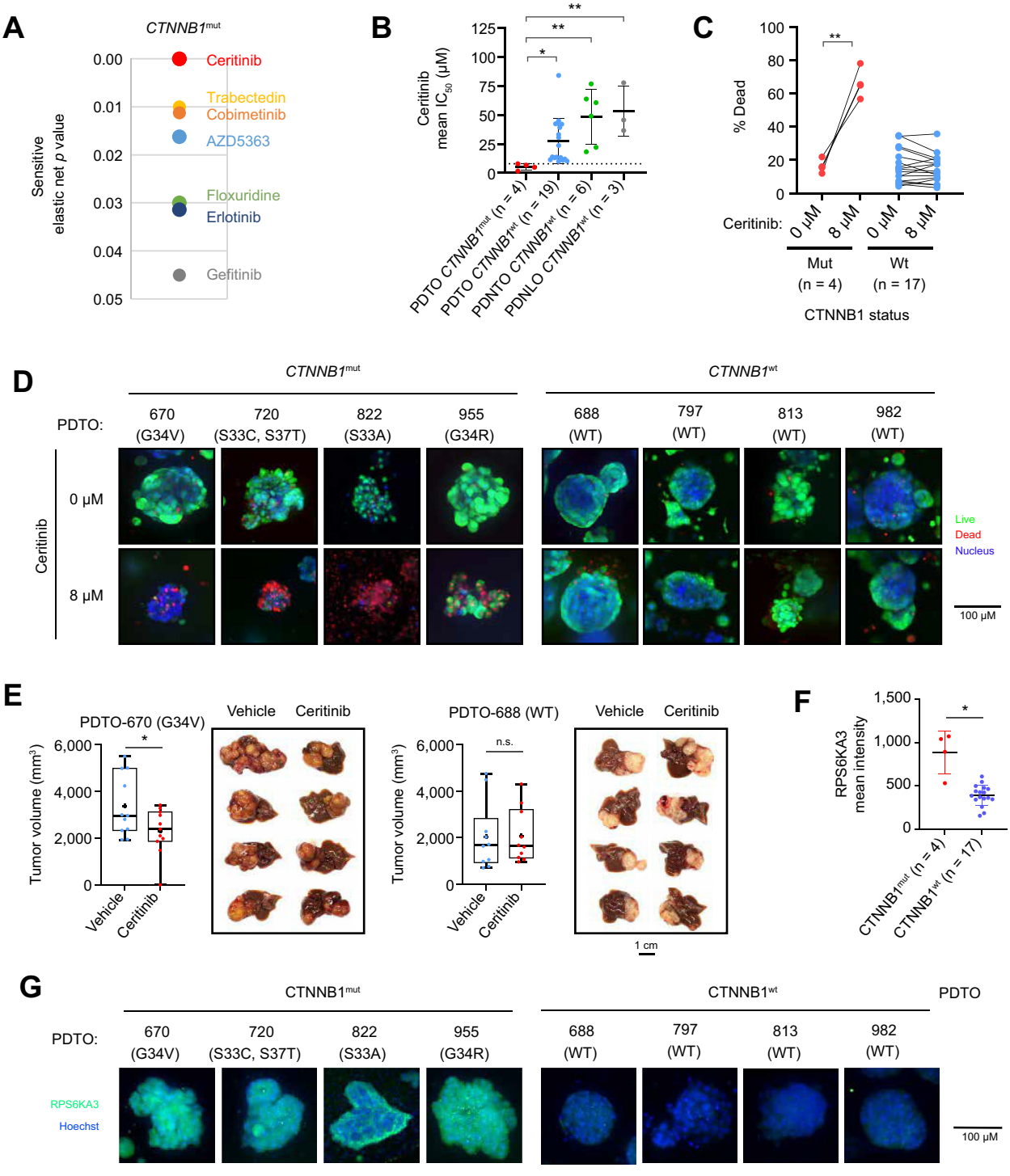


Fig. 3. *CTNNB1*^{mut} sensitivity towards ceritinib is independent of ALK. (A) Elastic net analysis for *CTNNB1*mut-specific sensitive drugs (p <0.05). (B) Scatterplot of ceritinib mean IC_{50} values grouped by *CTNNB1* mutation status and organoid type. (C) Live/dead high-content imaging quantification of PDTOs treated with or without ceritinib at IC_{50} concentration of 8 μM and (D) representative images from at least two experiments. (E) Tumor volumes (*left*) & representative images (*right*) of PDTOs orthotopically injected into NSG mice and treated with ceritinib (25 mg/kg) *p.o.* daily, five times a week, with 10–11 mice per treatment group. Statistical analysis by unpaired Student *t* test was deemed significant if *p <0.05. (F) High-content imaging quantification of RPS6KA3 in PDTOs grouped by *CTNNB1* mutation status. (G) Representative immunofluorescence high-content images of RPS6KA3. ALK, Anaplastic lymphoma kinase; *CTNNB1*, Catenin Beta-1 or Beta-catenin; Mut, Mutant; Catenin Beta-1 or Beta-catenin; Mut, Mutant; PDTO, patient-derived tumor organoid; *RPS6KA3, Ribosomal Protein S6 Kinase A3; Wt, wildtype*.

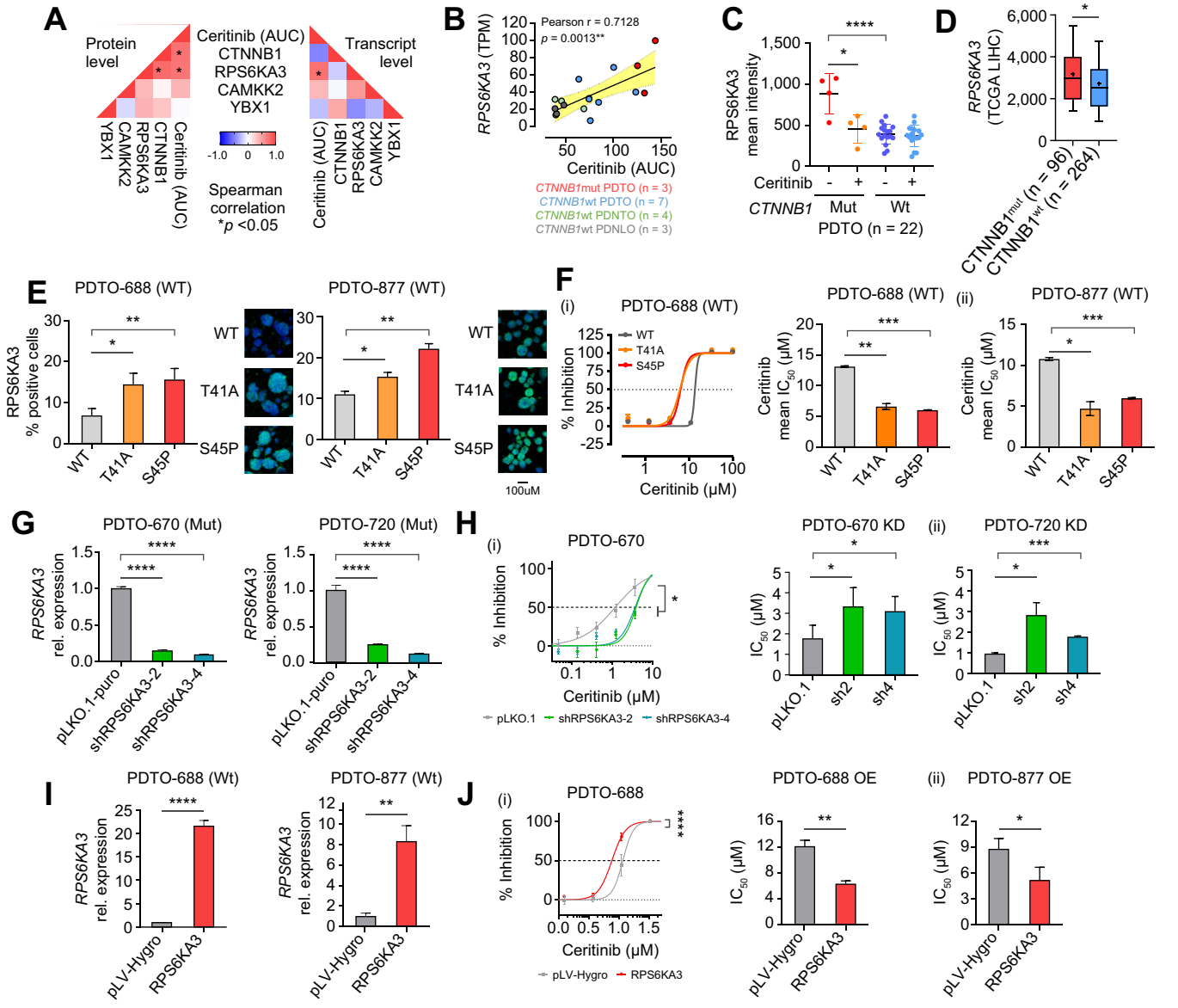


Fig. 4. A synthetic lethal link between *CTNNB1*mut and noncanonical NKD1-RPS6KA3 axis creates a therapeutic window for ceritinib. (A) Correlation matrix of ceritinib response (AUC) and polypharmacological targets at the protein and transcript levels. Spearman positive correlation, *p <0.05. (B) Correlation plot of *RPS6KA3* (TPM) and ceritinib response (AUC). Colors indicate *CTNNB1*mut status and PDO. (C) High-content imaging quantification of RPS6KA3 protein levels with (8 μM) or without (0 μM) ceritinib treatment (n = 2–3). (D) *RPS6KA3* expression in expanded LIHC TCGA cohort grouped by *CTNNB1* mutation status. (E) High-content imaging and quantification of RPS6KA3 protein levels by cell scoring analysis in two PDTOs stably overexpressing (OE) either WT, T41A, or S45P mutant *CTNNB1*. Mutations verified by Sanger sequencing. (F) Representative growth inhibition curve (*left*) and statistical analysis of ceritinib IC_{50} (*right*) (n = 2–3). (G) shRNA-mediated knockdown (KD) of *RPS6KA3* in *CTNNB1*mut PDTOs (PDTO-670 and PDTO-720) was validated by qPCR. Expression relative to 18s. (H) Representative growth inhibition curve (*left*) and statistical analysis of ceritinib IC_{50} (*right*) of *CTNNB1*mut PDTO-670 (i) and PDTO-720 (ii) after shRNA-mediated KD *RPS6KA3* (n = 3). (I) Overexpression (OE) of *RPS6KA3* in *CTNNB1*wt PDTOs (PDTO-688 and PDTO-877) was validated by qPCR. Expression relative to 18s. (J) Representative growth inhibition curve (*left*) and statistical analysis of ceritinib IC_{50} (*right*) of *CTNNB1*wt PDTO-688 (i) and PDTO-877 (ii) after OE of *RPS6KA3* (n = 3). *CTNNB1,* Catenin Beta-1 or Beta-catenin; PDO, patient-derived organoid; PDTO, patient-derived tumor organoid; *RPS6KA3,* Ribosomal Protein S6 Kinase A3; TPM, transcript per million.

CAMKK2 and YBX1. Indeed, we found a significantly elevated RPS6KA3 levels in all *CTNNB1*^{mut} PDTOs compared with the wildtype (Fig. 3F).

RPS6KA3 correlated with ceritinib response (AUC) at both the transcript and protein levels (Fig. 4A and B). PDTOs treated with ceritinib also led to inhibition of RPS6KA3 (Fig. 4C), which suggested the likelihood of RPS6KA3 as a downstream actionable target of ceritinib in the context of *CTNNB1*^{mut}. The *CTNNB1*mut-specific upregulation of *RPS6KA3* mRNA was also observed in an extended cohort of HCC (LIHC cohort) (Fig. 4D). We next tested the plausible synthetic lethality between mutant β-catenin and *RPS6KA3*. To demonstrate a direct link between *CTNNB1* mutation and RPS6KA3, we generated two isogenic PDTO models with wildtype *CTNNB1* (PDTO-688 and PDTO-877) that stably overexpress (OE) either *CTNNB1* wildtype, S45P, or T41A. These two mutations were

selected based on their highest occurring frequency in HCC.[22,28,42] We observed a spontaneous upregulation of RPS6KA3 in *CTNNB1* (S45P) and *CTNNB1* (T41A) compared with *CTNNB1* (wildtype) in both OE PDTO models (Fig. 4E). This also concurred with increased ceritinib sensitivity marked by the significantly lower IC_{50} in *CTNNB1* (S45P) and *CTNNB1* (T41A) compared with *CTNNB1* (wildtype) OE counterparts (Fig. 4E and F). Functionally, shRNA-mediated knockdown of *RPS6KA3* in *CTNNB1*^{mut} PDTOs (PDTO-670 and PDTO-720) caused spontaneous resistance to ceritinib (Fig. 4G and H). Conversely, stably overexpressing *RPS6KA3* in *CTNNB1*^{wt} PDTOs (PDTO-688 and PDTO-877) was able to sensitize *CTNNB1*^{wt} PDTOs to ceritinib (Fig. 4I and J).

To elucidate the potential underlying mechanism connecting mutant *CTNNB1* and *RPS6KA3* further, we defined genes that positively correlated with *RPS6KA3* in both PDTOs and a larger number of LIHC HCC tumors (p <0.05). Molecular Signatures Database (MSigDB) geneset enrichment analysis (GSEA) of 251

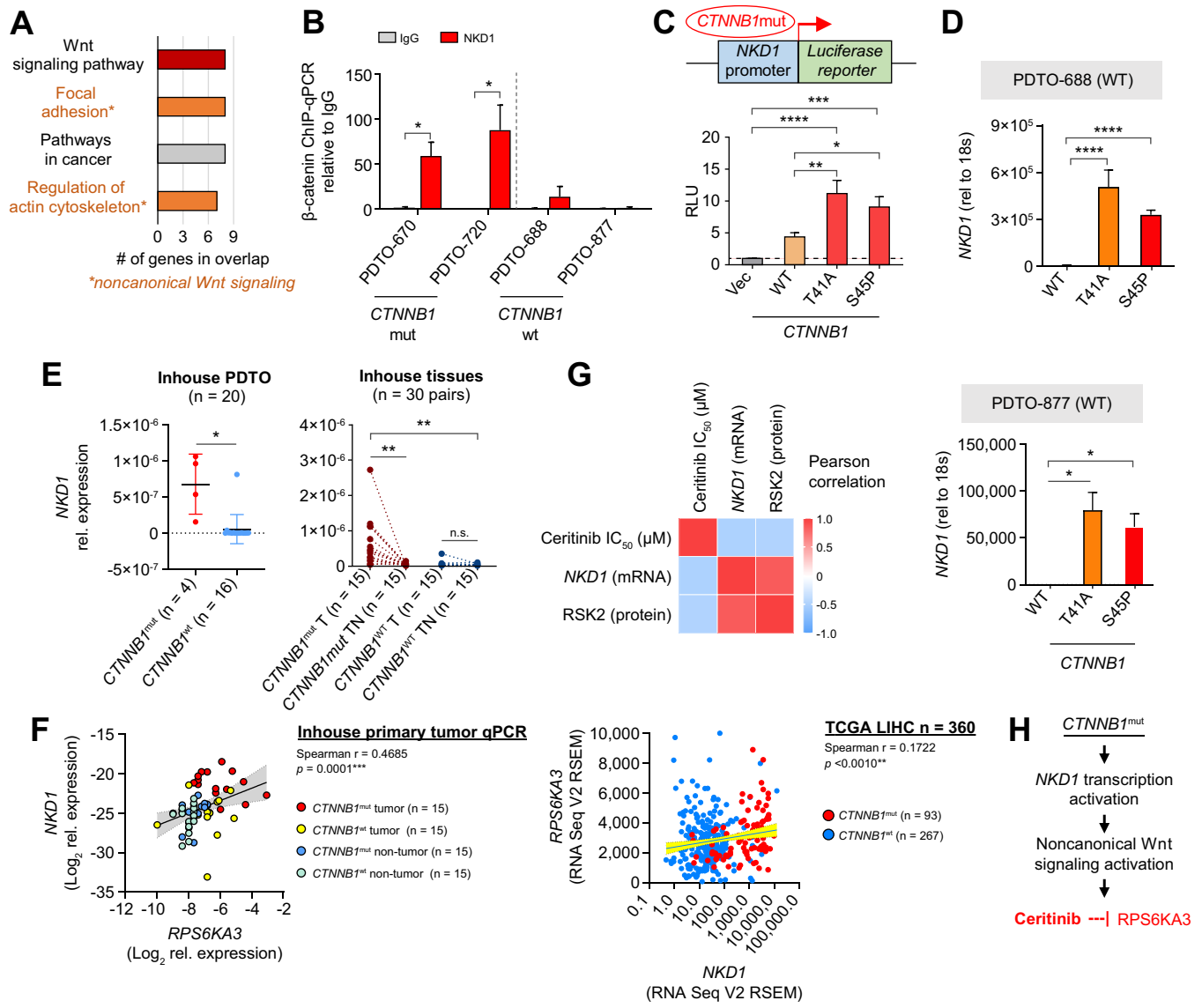


Fig 5. A synthetic lethal link between *CTNNB1*^{mut} and noncanonical NKD1-RPS6KA3 axis creates a therapeutic window for ceritinib. (A) KEGG functional clustering of 251 genes positively correlating with *RPS6KA3* in both in house PDTOs and in extended LIHC cohort. (B) ChIP-qPCR of β-catenin colocalization at *NKD1* promoter site shown relative to IgG. ChIP was performed in PDTOs harboring mutant (PDTO-670, PDTO-720) or wildtype (PDTO-688, PDTO-877) *CTNNB1*. (C) *NKD1* promoter reporter assay in 293FT showed activation by multiple hotspot mutations of *CTNNB1*. Relative luciferase unit (RLU) to vector control as detected by Dual-Glo luciferase. (D) qPCR-based quantification of *NKD1* mRNA expression in two PDTOs OE either WT, T41A, or S45P *CTNNB1* relative to endogenous control (18s). (E) qPCR-based quantification of *NKD1* mRNA expression relative to endogenous control (*18s*) in an expanded inhouse cohort of PDTOs (*left*) as well as inhouse paired T & TN tissues (*right*) grouped by *CTNNB1* mutation status. (F) Correlation plot between *NKD1* & *RPS6KA3* mRNA expression in inhouse cohort (*left*) as well as in extended LIHC cohort (n = 360) (*right*). (G) Pearson correlation matrix of ceritinib sensitivity (IC_{50}), *NKD1* mRNA (rel. to 18s) and RPS6KA3 protein expression (high-content imaging quantification by mean intensity) showing significant covariation in expanded panel of 23 PDTOs. (H) Diagrammatic summary of proposed mechanism underlying *CTNNB1*mut sensitivity to ceritinib. *CTNNB1,* Catenin Beta-1 or Beta-catenin; KEGG, Kyoto Encyclopedia of Genes and Genomes; *NKD1*, NKD Inhibitor of Wnt signaling pathway 1; PDTO, patient-derived tumor organoid; *RPS6KA3,* Ribosomal Protein S6 Kinase A3.

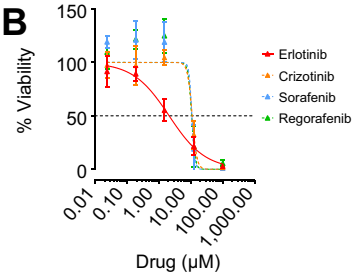
overlapping genes revealed that *RPS6KA3* strongly correlated with pathways associated with the non-canonical Wnt signaling (Fig. 5A). More specifically, the noncanonical arm involving planar cell polarity, where *NKD1* is an upstream regulator (Fig. S6D). We confirmed mutant β-catenin, but not wildtype, could directly bind to the *NKD1* promoter from chromatin immunoprecipitation-qPCR (Fig. 5B). Hotspot *CTNNB1*^{mut} S45P or T41A were able to activate promoter activity of *CTNNB1*^{mut}-bound *NKD1* region significantly, compared with the wildtype and vector (Fig. 5C). *CTNNB1*^{mut}-specific upregulation of *NKD1* was also observed in two PDTOs stably OE *CTNNB1* S45P and T41A mutations (Fig. 5D), and in endogenous PDTOs grouped by *CTNNB1*mut status (Fig. 5E). *NKD1* was also upregulated in an extended group of matching tumor and nontumor HCC tissues (Fig. 5E). A positive correlation between *NKD1* and *RPS6KA3* could also be established and showed concordance in the inhouse PDTOs, primary tissues and TCGA LIHC cohort (Fig. 5F and G). We hypothesize a synthetically lethal link between *CTNNB1*^{mut} and *RPS6KA3*/RSK2, whereby *NKD1*-mediated activation of noncanonical Wnt signaling leads to upregulation of ceritinib polypharmacological target RPS6KA3 (Fig. 5H).

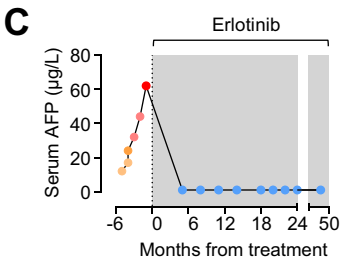
PDTO guided patient management

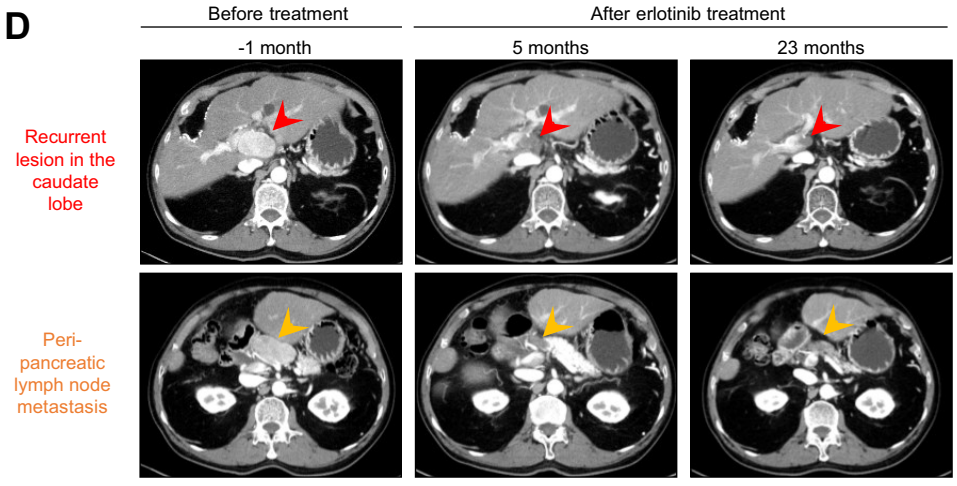
Despite significant medical advances, treatment of HCC remains a formidable challenge. We undertook a proof-of-concept study in using combined next-generation sequencing, PDTO culture, and testing of drugs selected based on genome-guided CVIs in the patient PDTO to create a personalized approach of systemic therapy in two patients with HCC. Both patients had reached late stage HCC with no further treatment options.

A

Patient variant	Target	Drug	Mean IC_{50} ± SD (μM)
EGFR gain	*EGFR*	Erlotinib	2.144 ± 0.59
MET gain	*MET*	Crizotinib	10.075 ± 1.789
FDA-approved for HCCT		Sorafenib	10.0155 ± 2.015
		Regorafenib	10.74 ± 0.113

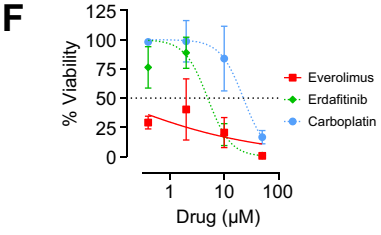






E

Patient variant	Target	Drug	Mean IC_{50} ± SD (μM)
TSC2^{E1583*}	mTOR	Everolimus	0.071 ± 0.008
FGFR1 gain	FGFR	Erdafitinib	6.139 ± 2.538
GSTP1^{I105V}	DNA / RNA synthesis	Carboplatin	15.605 ± 5.678



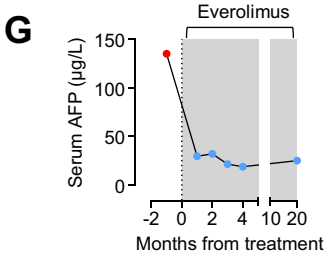


Fig. 6. A proof-of-concept study on PDTO-guided patient management. (A) Case 1 summary table of WES genome-guided clinical variant indication (CVI). (B) Growth inhibition curve for erlotinib, crizotinib, sorafenib, and regorafenib. (C) Serum AFP levels before and during course of erlotinib treatment. (D) CT scans of Case 1 before and after erlotinib treatment. (E) Case 2 summary table of WES genome-guided CVI. (F) Growth inhibition curve for everolimus, erdafitinib and carboplatin. (G) Serum AFP levels before and during the course of everolimus treatment. AFP, alpha-fetoprotein; PDTO, patient-derived tumor organoid; WES, whole-exome sequencing.

The first patient was a 70-year-old male with postoperative recurrent HCC failed transcatheter arterial chemoembolization, who underwent radiofrequency ablation, with first-line sorafenib and pembrolizumab immunotherapy. Progressive disease was shown with peri-pancreatic lymph node and high serum alpha-fetoprotein (AFP) level (62 μg/L) at the time of receiving PDTO-guided drug choice. Whole-genome sequencing showed a number of non-actionable missense mutations but we were able to identify potential actionable targets *EGFR* (erlotinib) and *MET* (crizotinib) from broad chr.7 amplification (Fig. 6A). PDTOs were subjected to single-agent drug testing against erlotinib (*EGFR* inhibitor),[43] crizotinib (*MET* inhibitor),[44,45] regorafenib (second-line treatment of HCC) and sorafenib for comparison because of known history of resistance. Growth inhibition curves suggested PDTO to be most sensitive to erlotinib at a mean IC_{50} of 2.144 ± 0.59 μM (Fig. 6A and B). Based on the predicted sensitivity, the patient started on daily TARCEVA® (erlotinib) in January 2020. Reassessment CT scan imaging showed no viable tumor after 5 months on TARCEVA® and treatment response persisted over a period of 48 months. The serum AFP level also returned to baseline and loss of peri-pancreatic lymph node involvement was also apparent at 5 months post-treatment (Fig. 6C and D). The patient is still in clinical complete remission in January 2024.

For the second case study, a 61-year-old male with advanced stage HCC received first and second treatments of immunotherapy and chemotherapy for his progressive disease. At the time of receiving PDTO-guided drug treatment he had also pulmonary metastases. SNV and CNV findings from WES were suggestive of potential actionable targets such as everolimus against *TSC2* p.E1583* (VAF 64.67%) and erdafitinib against *FGFR1* copy number gain (Fig. 6E). Carboplatin was also selected because of a germline single nucleotide polymorphism suggestive of platinum-based chemo-sensitivity to *GSTP1* p.I105V as reported in colorectal and lung cancers (Fig. 6E).[46,47] Growth inhibition curves suggested that everolimus was the most sensitive drug against PDTOs with a mean IC_{50} of 0.071 ± 0.008 μM (Fig. 6F). Subsequently, the patient was treated with everolimus and began to show partial response in 5 months based on his serum AFP levels returning to reference level (Fig. 6G). The patient continues to be well at 20 months, with stable disease and AFP below reference range in January 2025 (Fig. 6G).

Discussion

PDTOs are a reliable model for preclinical and translational studies. Despite positive retrospective correlations with patient response data, challenges such as culture success, cost, standardization, and time constraints hinder their clinical utility in guiding precision medicine. We have established a protocol using baseline culture media without growth factors or conditioned media commonly used in organoid establishment in an effort to minimize confounding factors during drug screen and environmental niche dependency.[13,19,20] It is also worth noting that although other studies have failed to grow grade I/II HCCs as organoids,[18] our protocol enabled a relatively higher efficiency of low-grade cultures. We observed that the use of growth factor-rich GF++ medium could lead to outgrowth of non-malignant organoids or fibroblasts that outcompeted the initially slow growing tumor clusters. Nevertheless, the use of growth factors has been beneficial in culturing cases with low cell viability in the starting material. For our proposed growth factor-low GF- medium, it is plausible that genomic factors of most HCC tumors could suffice the need to support cell growth through autocrine and/or paracrine signaling, thus negating the requirement for extra growth factors. Similar to our findings, prior work in colon and rectal cancer also suggested PDTOs could be cultured in the absence of key growth factors[48,49] (*e.g.* R-spondin, Wnt-3a and Noggin), whereas organoids derived from normal rectal mucosa remained growth factor dependent.[50] Overall, the reduced reliance on such components is also an important step towards standardization, and cost reduction – a major challenge in making PDTOs accessible and scalable for clinical implementation in the future.

Growing evidence suggests that genomically defined targets have an increased success rate in clinical development.[51–53] Indeed, the added value of PDTO screening to designing precision medicine approaches remain unclear for HCC. Recent genomic-driven strategy from Limousin *et al.*,[5] demonstrated clinical benefit of targeted treatment in three of 19 patients.[5] Genetic alterations in this study were classified according to the ESMO scale for clinical actionability for molecular targets (ESCAT).[4] However, it is worth noting that there are no indications above ESCAT III (hypothetical target) for HCC.[4,5] At best, these alteration-drug matches are suspected to improve outcome based on clinical trial in other tumor types with similar molecular alteration, the status of which is unknown in HCC.[4] In such context, PDTO drug screening may prove useful in evaluating response *ex vivo*. More importantly, the patient genomic profile may present with more than one potentially actionable target with similar ESCAT ranking at IIIa/b, as was also observed in the Limousin *et al.*[5] study. In which case, pre-screening in *ex vivo* models such as PDTOs can also aid in candidate prioritization. We have encountered this first-hand and presented two case studies as proof-of-concept that genomic-driven strategy supported by PDTO screen-guided management results in clear patient benefit. Our study presents two exemplary cases that not only substantiate the feasibility of utilizing PDTOs to predict patient response, but also underscore their potential in guiding treatment decisions for patients with HCC. In our hands, the expedited process from receiving the biopsy, WES, to delivering the PDTO drug test results was completed within 20 days without sacrificing the quality of results. This provides a proof of principle of the shortest feasible time frame that can be achieved for pharmacogenomic-guided PDTO testing and how it may fit within the clinical setting. Clinical trials expanding the cohort of HCC patients as well as development of assays that include immunotherapeutic drugs are warranted and within reach.[54,55] Future development of drug testing systems that recapitulate the tumor-microenvironment interplay such as whether the presence of fibroblasts/endothelial cells would also affect angiogenesis inhibitor efficacy *ex vivo*, would also address a key limitation of our existing platform.

In spite of the constraints imposed by the limited sample size, our study successfully achieved a proportionate representation and resolution concerning both loss and gain of function properties associated with HCC driver mutations. This enabled the identification of potential actionable strategies for previously deemed undruggable mutations, expanding the

horizons for therapeutic interventions in HCC. We showed in our cohort of PD-tumor, nontumor, and normal liver-derived organoids that there are indeed many FDA-approved drugs, including those approved for HCC showing lack of tumor specificity. Therapeutic index of these drugs such as lenvatinib could be improved via pharmacogenomic based stratification (*i.e.* by *TP53* missense mutation status). However, this is not always possible as many CVIs are associated with passenger events instead of driver mutations of high incidence. Out of the 100 drugs tested, only 19 showed tumor specificity in PDTOs. Interestingly, several of them are targeted therapies with well-known CVIs, such as ceritinib. However, their linked genetic variants are generally not found in HCC, which may explain in part the lack of clinical trial information on ceritinib in HCC. For instance, ALK fusion or upregulation indicative of ceritinib sensitivity are not found in HCC. Instead, EN regression linked ceritinib to mutant *CTNNB1*. ROC analysis supports the possibility of using *CTNNB1* mutation status (VAF >0.2) or RSK2 protein level as biomarkers for stratifying patients who may benefit from ceritinib treatment (Fig. S6E). Although we used high-content systems to quantify RSK2 protein levels, the detection method can in theory also be adapted for immunohistochemistry, which is more accessible in the clinical setting. However, the use of somatic mutation (VAF) is more robust as a biomarker because of its higher tumor specificity. Existing FDA-approved genomic profiling panels such as FoundationOne CDx already test for *CTNNB1* so clinical implementation is indeed within reach. In line with the role of RSK2 in MAPK signaling, it is also worth noting that *CTNNB1*mut PDTOs also responded to MAPK inhibitor cobimetinib, albeit at a less *CTNNB1*mut-specific manner compared to ceritinib (Fig. 3A, Fig. S6F, Table S8). Overall, stratifying patient subpopulation for tumor presence of *CTNNB1* mutations may offer, for the first time, an outlook on a treatment and allow assignment into new clinical trials on repurposing an FDA-approved drug to HCC.

Disproportionate representation of *CTNNB1* mutations in existing HCC cell lines (1/22, 4.5% based on the latest Cancer Cell Line Encyclopedia [CCLE])[56] and patient-derived tumor organoid cohorts (1/40, 2.5% based on Ji *et al.*;[17] 2/32, 6.25% based on Yang *et al.*[14]) has restricted efforts on studying the synthetic lethal component linked therapy for this undruggable driver event of HCC.[57–59] Our pharmacogenomic analysis on $CTNNB1^{mut}$ PDTOs and functional investigations revealed that $CTNNB1^{mut}$/*NKD1*-associated activation of noncanonical Wnt signaling can lead to ceritinib sensitivity via upregulation of the polypharmacological target RPS6KA3. Like other pharmacogenomic CVIs, the mutation status of the downstream targets themselves (such as *RPS6KA3*) within the synthetic lethal network governed by a driver mutation (such as *CTNNB1*) need to be taken into consideration. Of note, *RPS6KA3* somatic alterations significantly co-occurred with *AXIN1* (p <0.0001) instead of *CTNNB1* mutations (p = 0.564) (Fig. S7A and B), which also echoed the findings of Schaeffer *et al.*[60] In addition to significant mutual exclusivity between *AXIN1* and *CTNNB1* mutations (Fig. S7B), the underlying transcriptomic signature for these two mutations also differ suggesting that β-catenin activation via *AXIN1* loss may not lead to the same events as *CTNNB1* mutations.[37] Indeed, we observed significant *RPS6KA3* upregulation in *CTNNB1* mutant *vs.* wildtype HCC, but not when grouped by *AXIN1* mutation status (Fig. S7C). Given that *RPS6KA3* also has tumor suppressive properties,[60] further investigation is needed to fully understand the underlying synthetic lethality between $CTNNB1^{mut}$ and ceritinib.

In sum, our study poised to provide an optimized protocol aimed at enhancing the success rate of HCC organoid establishment. Our results open up new avenues of clinical trial investigations to elucidate the link between variant–drug pairs and the wider utilization of PDTOs in precision medicine, thereby advancing the field towards more effective and personalized therapeutic approaches.

Affiliations

[1]*Department of Surgery, Sir YK Pao Centre for Cancer, The Chinese University of Hong Kong, Shatin, Hong Kong, China;* [2]*State Key Laboratory of Digital Medical Engineering, School of Biomedical Science and Medicinal Engineering, Southeast University, Nanjing, China;* [3]*Department of Anatomical and Cellular Pathology, The Chinese University of Hong Kong, Shatin, Hong Kong, China;* [4]*Department of Biomedical Sciences, Faculty of Health Sciences, University of Macau, Taipa, Macao, China;* [5]*Department of Clinical Oncology, The Chinese University of Hong Kong, Shatin, Hong Kong, China*

Abbreviations

AFP, alpha-fetoprotein; ALK, anaplastic lymphoma kinase; ATCC, American Type Culture Collection; CNV, copy number variation; CTNNB1, beta-catenin; CVI, clinical variant indicator; EN, elastic net; GF, growth factor; HCC, hepatocellular carcinoma; IF, immunofluorescence; KEGG, Kyoto Encyclopedia of Genes and Genomes; MSigDB, Molecular Signatures Database; OE, overexpress; PCA, principal component analysis; PD, patient-derived; PDNL, patient-derived normal liver; PDNLO, patient-derived normal liver organoid; PDNT, patient-derived adjacent nontumor; PDNTO, patient-derived nontumor organoid; PDO, patient-derived organoid; PDT, patient-derived tumor; PDTO, patient-derived tumor organoid; PDTCL, patient-derived tumor cell line; RPS6KA3, Ribosomal Protein S6 Kinase A3; SNV, somatic nucleotide variant; TCGA, The Cancer Genome Atlas; TPM, transcript per million; VAF, variant allele frequency; WES, whole-exome sequencing.

Financial support

This work was supported by the Hong Kong Research Grants Council (RGC) Research Impact Fund (Ref. R4017-18), RGC Area of Excellence Scheme (Ref. AoE/M-401/20) and a Direct Grant for Research from the Chinese University of Hong Kong (CUHK). This research is also in part supported by a US National Institutes of Health RO1 fund (Ref. R01CA229836) and a Hong Kong ITF Partnership Research Programme (Ref. PRP/073/21FX).

Conflicts of interest

The authors declare no competing financial interests.

Please refer to the accompanying ICMJE disclosure forms for further details.

Authors' contributions

Performed biological experiments, drug screening, analyzed and interpreted data: AlissaMW, AikhaMW. Prepared and wrote the manuscript: AlissaMW, AikhaMW, NW. Conducted bioinformatic analysis of WES and transcriptome, and mapping of gene–drug associations: HH, XD, XW. Propagated patient specimens for organoids and monolayer cultures, prepared samples for sequencing, staining and drug screens, and xenotransplantation: WWC, AMW, HYL, LZ, CC, CKC. Performed histological examination of patient–organoid pairs: HHL, AWC. Provided patient materials and associated clinical annotations: YL, KCN. Clinical management of patient treated with drug found from organoid result: SLC. Conceived and supervised the study: NW.

Data availability statement

Study materials such as organoids generated in this study are available from the lead contact with a completed Materials Transfer Agreement. There are restrictions on the availability of PDOs because of the lack of an external centralized repository for its distribution and our need to maintain the stock. We are glad to share with

reasonable compensation by requestor for its processing and shipping. Datasets and analytic methods used during the current study are available in the Supplementary Tables. Public HCC datasets from the TCGA were downloaded from cBioportal. Standardized codes used in this study are also described under the Method Details section. Further information and requests should be directed to and will be fulfilled by the lead contact, Nathalie Wong (natwong@cuhk.edu.hk).

Acknowledgements

The authors thank the Core Utilities of Cancer Genomics and Pathobiology (CUHK) and the Microscopy & Imaging Core of the School of Biomedical Sciences (CUHK) for providing the facilities to support this research. We also thank Chow Chit, Maggie Cheung, Matthew Man, Hui Chen, Mian He, Jianqing Yu, and Dandan Pu for technical assistance.

Supplementary data

Supplementary data to this article can be found online at https://doi.org/10.1016/j.jhepr.2025.101426.

References

Author names in bold designate shared co-first authorship

[1] Yang JD, Hainaut P, Gores GJ, et al. A global view of hepatocellular carcinoma: trends, risk, prevention and management. Nat Rev Gastroenterol Hepatol 2019;16:589–604.
[2] Sung H, Ferlay J, Siegel RL, et al. Global Cancer Statistics 2020: GLOBOCAN estimates of incidence and mortality worldwide for 36 cancers in 185 countries. CA Cancer J Clin 2021;71:209–249.
[3] **Griffith M**, **Spies NC**, **Krysiak K**, et al. CIViC is a community knowledgebase for expert crowdsourcing the clinical interpretation of variants in cancer. Nat Genet 2017;49:170–174.
[4] Mateo J, Chakravarty D, Dienstmann R, et al. A framework to rank genomic alterations as targets for cancer precision medicine: the ESMO Scale for Clinical Actionability of molecular Targets (ESCAT). Ann Oncol 2018;29:1895–1902.
[5] Limousin W, Laurent-Puig P, Ziol M, et al. Molecular-based targeted therapies in patients with hepatocellular carcinoma and hepatocholangiocarcinoma refractory to atezolizumab/bevacizumab. J Hepatol 2023;79:1450–1458.
[6] Zucman-Rossi J, Villanueva A, Nault JC, et al.. Genetic landscape and biomarkers of hepatocellular carcinoma. Gastroenterology 2015;149:1226–1239.e4.
[7] Kennedy MC, Lowe SW. Mutant p53: it's not all one and the same. Cell Death Differ 2022;29:983–987.
[8] Kahn M. Can we safely target the WNT pathway? Nat Rev Drug Discov 2014;13:513–532.
[9] Pushpakom S, Iorio F, Eyers PA, et al. Drug repurposing: progress, challenges and recommendations. Nat Rev Drug Discov 2018;18:41–58.
[10] Corsello SM, Bittker JA, Liu Z, et al. The Drug Repurposing Hub: a next-generation drug library and information resource. Nat Med 2017;23:405–408.
[11] Wensink GE, Elias SG, Mullenders J, et al. Patient-derived organoids as a predictive biomarker for treatment response in cancer patients. Npj Precis Oncol 2021;5:30.
[12] Clevers H. Modeling development and disease with organoids. Cell 2016;165:1586–1597.
[13] Veninga V, Voest EE. Tumor organoids: opportunities and challenges to guide precision medicine. Cancer Cell 2021;39:1190–1201.
[14] **Yang H**, **Cheng J**, **Zhuang H**, et al. Pharmacogenomic profiling of intra-tumor heterogeneity using a large organoid biobank of liver cancer. Cancer Cell 2024;42:535–551.
[15] Broutier L, Mastrogiovanni G, Verstegen MMA, et al. Human primary liver cancer-derived organoid cultures for disease modeling and drug screening. Nat Med 2017;23:1424–1435.
[16] Nuciforo S, Fofana I, Matter MS, et al. Organoid models of human liver cancers derived from tumor needle biopsies. Cell Rep 2018;24:1363–1376.
[17] **Ji S**, **Feng L**, **Fu Z**, et al. Pharmaco-proteogenomic characterization of liver cancer organoids for precision oncology. Sci Transl Med 2023;15:eadg3358.
[18] **van Tienderen GS**, **Li L**, **Broutier L**, et al. Hepatobiliary tumor organoids for personalized medicine: a multicenter view on establishment, limitations, and future directions. Cancer Cell 2022;40:226–230.
[19] LeSavage BL, Suhar RA, Broguiere N, et al. Next-generation cancer organoids. Nat Mater 2022;21:143–159.
[20] **Nanki K**, **Toshimitsu K**, **Takano A**, et al. Divergent routes toward Wnt and R-spondin niche independency during human gastric carcinogenesis. Cell 2018;174:856–869.e17.
[21] **Lam YK**, **Yu J**, Huang H, et al. TP53 R249S mutation in hepatic organoids captures the predisposing cancer risk. Hepatology 2023;78:727–740.
[22] **Wong AM**, **Ding X**, Wong AM, et al. Unique molecular characteristics of NAFLD-associated liver cancer accentuate β-catenin/TNFRSF19-mediated immune evasion. J Hepatol 2022;77:410–423.
[23] Friedman J, Hastie T, Tibshirani R. Regularization paths for generalized linear models via coordinate descent. J Stat Softw 2010;33:1–22.
[24] Metsalu T, Vilo J. ClustVis: a web tool for visualizing clustering of multivariate data using principal component analysis and heatmap. Nucleic Acid Res 2015;1(43):W566–W570.
[25] **Marsee A**, **Roos FJM**, Verstegen MMA, et al. Building consensus on definition and nomenclature of hepatic, pancreatic, and biliary organoids. Cell Stem Cell 2021;28:816–832.
[26] **Acanda De La Rocha AM**, **Berlow NE**, Fader M, et al. Feasibility of functional precision medicine for guiding treatment of relapsed or refractory pediatric cancers. Nat Med 2024;30:990–1000.
[27] **Ding X**, **He M**, Chan AWH, et al. Genomic and epigenomic features of primary and recurrent hepatocellular carcinomas. Gastroenterology 2019;157:1630–1645.e6.
[28] Ally A, Balasundaram M, Carlsen R, et al. Comprehensive and integrative genomic characterization of hepatocellular carcinoma. Cell 2017;169:1327–1341.e23.
[29] Pang E, Wong N, Lai PBS, et al.. Consistent chromosome 10 rearrangements in four newly established human hepatocellular carcinoma cell lines. Genes Chromosom Cancer 2002;33:150–159.
[30] Gho JWM, Ip WK, Chan KYY. et al. Re-expression of transcription factor ATF5 in hepatocellular carcinoma induces G2-M arrest. Cancer Res 2008;68:6743–6751.
[31] Tiniakos DG, Vos MB, Brunt EM. Nonalcoholic fatty liver disease: pathology and pathogenesis. Annu Rev Pathol Mech Dis 2010;5:145–171.
[32] Heid HW, Moll R, Schwetlick I, et al. Adipophilin is a specific marker of lipid accumulation in diverse cell types and diseases. Cell Tissue Res 1998;294:309–321.
[33] Straub BK, Gyoengyoesi B, Koenig M, et al. Adipophilin/perilipin-2 as a lipid droplet-specific marker for metabolically active cells and diseases associated with metabolic dysregulation. Histopathology 2013;62:617–631.
[34] Pirmohamed M. Pharmacogenomics: current status and future perspectives. Nat Rev Genet 2023;24:350–362.
[35] **Rodon J**, **Tawbi HA**, Thomas AL, et al. A phase I, multicenter, open-label, first-in-human, dose-escalation study of the oral smoothened inhibitor sonidegib (LDE225) in patients with advanced solid tumors. Clin Cancer Res 2014;20:1900–1909.
[36] Abou-Alfa GK, Meyer T, Cheng A-L, et al. Cabozantinib in patients with advanced and progressing hepatocellular carcinoma. N Engl J Med 2018;379:54–63.
[37] Llovet JM, Kelley RK, Villanueva A, et al. Hepatocellular carcinoma. Nat Rev Dis Prim 2021;7:1–28.
[38] de Andrade KC, Lee EE, Tookmanian EM, et al. The TP53 Database: transition from the International Agency for Research on Cancer to the US National Cancer Institute. Cell Death Differ 2022;29:1071–1073.
[39] Wheler JJ, Janku F, Naing A, et al. TP53 alterations correlate with response to VEGF/VEGFR inhibitors: implications for targeted therapeutics. Mol Cancer Ther 2016;15:2475–2485.
[40] Shaw AT, Kim TM, Crinò L, et al. Ceritinib versus chemotherapy in patients with ALK-rearranged non-small-cell lung cancer previously given chemotherapy and crizotinib (ASCEND-5): a randomised, controlled, open-label, phase 3 trial. Lancet Oncol 2017;18:874–886.
[41] Kuenzi BM, Remsing Rix LL, Stewart PA, et al. Polypharmacology-based ceritinib repurposing using integrated functional proteomics. Nat Chem Biol 2017;13:1222–1231.
[42] **Schulze K**, **Imbeaud S**, **Letouzé E**, et al. Exome sequencing of hepatocellular carcinomas identifies new mutational signatures and potential therapeutic targets. Nat Genet 2015;47:505–511.
[43] Tsao M-S, Sakurada A, Cutz J-C, et al. Erlotinib in lung cancer — molecular and clinical predictors of outcome. N Engl J Med 2005;353:133–144.
[44] Landi L, Chiari R, Tiseo M, et al. Crizotinib in MET-deregulated or ROS1-rearranged pretreated non–small cell lung cancer (METROS): a phase II, prospective, multicenter, two-arms trial. Clin Cancer Res 2019;25:7312–7319.

[45] **Lennerz JK**, **Kwak EL**, **Ackerman A**, et al. MET amplification identifies a small and aggressive subgroup of esophagogastric adenocarcinoma with evidence of responsiveness to crizotinib. J Clin Oncol 2011;29:4803–4810.
[46] Shen X, Wang J, Yan X, et al. Predictive value of GSTP1 Ile105Val polymorphism in clinical outcomes of chemotherapy in gastric and colorectal cancers: a systematic review and meta-analysis. Cancer Chemother Pharmacol 2016;77:1285–1302.
[47] Ye H, Shao M, Shi X, et al. Predictive assessment in pharmacogenetics of Glutathione S-transferases genes on efficacy of platinum-based chemotherapy in non-small cell lung cancer patients. Sci Rep 2017;7:2760.
[48] **Van De Wetering M**, **Francies HE**, **Francis JM**, et al. Prospective derivation of a living organoid biobank of colorectal cancer patients. Cell 2015;161:933–945.
[49] **Ganesh K**, **Wu C**, O'Rourke KP, et al. A rectal cancer organoid platform to study individual responses to chemoradiation. Nat Med 2019;25:1607–1614.
[50] Sato T, Stange DE, Ferrante M, et al. Long-term expansion of epithelial organoids from human colon, adenoma, adenocarcinoma, and Barrett's epithelium. Gastroenterology 2011;141:1762–1772.
[51] Hay M, Thomas DW, Craighead JL, Economides C, Rosenthal J. Clinical development success rates for investigational drugs. Nat Biotechnol 2014;32:40–51.
[52] King EA, Wade Davis J, Degner JF. Are drug targets with genetic support twice as likely to be approved? Revised estimates of the impact of genetic support for drug mechanisms on the probability of drug approval. PLoS Genet 2019;15:e1008489.
[53] Plenge RM, Scolnick EM, Altshuler D. Validating therapeutic targets through human genetics. Nat Rev Drug Discov 2013;12:581–594.
[54] **Neal JT**, **Li X**, Zhu J, et al. Organoid modeling of the tumor immune microenvironment. Cell 2018;175:1972–1988.e16.
[55] **Voabil P**, **de Bruijn M**, **Roelofsen LM**, et al. An ex vivo tumor fragment platform to dissect response to PD-1 blockade in cancer. Nat Med 2021;27:1250–1261.
[56] **Ghandi M**, **Huang FW**, Jané-Valbuena J, et al. Next-generation characterization of the cancer cell line Encyclopedia. Nature 2019;569:503–508.
[57] **Barretina J**, **Caponigro G**, **Stransky N**, et al. The Cancer Cell Line Encyclopedia enables predictive modelling of anticancer drug sensitivity. Nature 2012;483:603–607.
[58] **Iorio F**, **Knijnenburg TA**, **Vis DJ**, et al. A landscape of pharmacogenomic interactions in cancer. Cell 2016;166:740–754.
[59] **Tsherniak A**, **Vazquez F**, Montgomery PG, et al. Defining a cancer dependency map. Cell 2017;170:564–576.e16.
[60] **Schaeffer S**, **Gupta B**, **Calatayud AL**, et al. RSK2 inactivation cooperates with AXIN1 inactivation or β-catenin activation to promote hepatocarcinogenesis. J Hepatol 2023;79:704–716.

Keywords: Liver cancer organoids; Drug repurposing; Precision medicine; *CTNNB1*; Synthetic lethality.
Received 22 January 2025; received in revised form 8 April 2025; accepted 9 April 2025; Available online 22 April 2025